

**FREQUENCIES AND MODES
OF ROTATING FLEXIBLE SHROUDED
BLADED DISCS-SHAFT ASSEMBLIES**
JACEK SOKOŁOWSKI¹, ROMUALD RZĄDKOWSKI^{1,2}
AND LESZEK KWAPISZ¹

¹*Department of Dynamics of Machines,
Institute of Fluid Flow Machinery, Polish Academy of Sciences,
J. Fiszer 14, 80-952 Gdansk, Poland
{jsokolow,z3,kwapi}@imp.gda.pl*

²*Polish Naval Academy,
Śmidowicza 71, 81-919 Gdynia, Poland*

(Received 26 November 2002; revised manuscript received 6 December 2002)

Abstract: It is now increasingly necessary to predict accurately, at the design stage and without excessive computing costs, the dynamic behaviour of rotating parts of turbomachines, so that resonant conditions at operating speeds are avoided. In this study, global rotating mode shapes of flexible shrouded bladed disc-shaft assemblies are calculated. The rotating modes have been calculated by using a finite element cyclic symmetry approach. Rotational effects, such as centrifugal stiffening have been accounted for, and all the possible couplings between the flexible parts have been allowed. Gyroscopic effects have been neglected. The numerical results have been compared with the experimental. The calculations show the influence of shaft flexibility on the natural frequencies of shrouded bladed discs up to four nodal diameters for the two first frequencies series.

Keywords: blades, discs, shaft, free vibration

1. Introduction

Fatigue failure of rotor blades is one of the most serious problems faced by the designers of modern aircraft gas turbine engines. To come up with a successful design, the engineer needs to predict accurately resonance and instability regions, which must be avoided during operation. If such dangerous, aerodynamically induced vibrations are not predicated at an early stage of a design, and are discovered only after the system has been developed, tremendous resources will be consumed in redesigning it. Although the stability problem is still of great concern, it is not addressed here. The present work deals with the free vibration of the shrouded bladed disc placed on the part of the shaft.

Two independent approaches are commonly used to analyse the dynamic behaviour of turbomachinery rotating assemblies. On the one hand, the rotordynamics

approach is concerned with disc-shaft systems. The shaft is mostly modelled by using beam finite elements, and disc flexibility is not considered in some works [1–4], while it is considered in others [4–8]. On the other hand, the bladed-disc approach deals with flexible discs [9–11]. The disc-shaft attachment is assumed to be rigid, the inertial effects generated by the shaft displacements are disregarded, and the gyroscopic effects usually neglected. Many efficient models have been developed over the years in these two basic approaches. However, there is growing evidence that, when a flexible-bladed disc is mounted on a flexible shaft, the resulting system may have vibration characteristics that depend on the coupling between the vibration modes of the individual components.

Loewy and Khader [12] analyzed the influence of shaft flexibility on the one-nodal diameter frequencies of bladed discs. The model is based on the natural vibration modes of the non-rotating disc with a rigid hub, used as generalised coordinates in a small-perturbation Lagrangian formulation. Shaft flexibility is represented by translational and rotational springs acting at the centre of the disc. The quasi-steady aerodynamic loading was included in Khader and Loewy [13], where they have evaluated its effect on the forced response of the system. Khader and Masoud [14] also developed an analytical model in order to achieve better assessment of blade mistuning effects on the free vibration characteristics of non-rotating flexible-blade, rigid-disc and flexible-shaft assemblies. They improved the traditional model by introducing a continuous shaft model, thus providing a more realistic representation of shaft flexibility. Dubigeon and Michon [6] also improved the non-rotating flexible-blade, rigid-disc, flexible-shaft model by introducing a finite-element representation of the blades. Shahab and Thomas [8] used the finite element method with a special thick three-dimensional element and a cyclic symmetry formulation to study the coupling effect of disc flexibility on the dynamic behaviour of non-rotating multi-disc shaft systems. All these models have been useful for establishing and illustrating the influence of coupling effects in blade-disc-shaft systems. However, they are based on simplified formulations and cannot be easily applied to a wide range of realistic structures. Therefore, to analyse the whole flexible blade-disc-shaft assembly of real structures, efficient reduction techniques have to be proposed and assessed. The formulation presented by Richardet *et al.* [15] is based on global analysis of rotating assemblies modelled with finite elements. The undamped non-rotating system is first analysed by using the wave propagation method associated with a component mode reduction. Then, the whole system submitted to centrifugal and gyroscopic effects is analysed after a modal reduction. An application to a steel impeller mounted on a shaft shows the capacity of the method to compute accurately and efficiently the frequencies and mode shapes of rotating industrial structures, and points out the differences encountered when using various modelling methods.

In this paper, the natural frequencies of a rotating single shrouded bladed disc of a steam turbine, a shrouded bladed disc placed on the part of a shaft, as well as those of two and three shrouded bladed discs placed on the part of a shaft are presented. The calculations show the influence of the shaft on the natural frequencies of the shrouded bladed discs up to four nodal diameter frequencies for the two first frequencies group.

2. Description of the model

The ABAQUS finite element code is used for structural and dynamic analyses. Valuable experience is available and, therefore, the ABAQUS program was integrated into the design procedure.

Disc assemblies containing N turbine blades coupled circumferentially through the elastic rotor had to be analysed. Blade mistuning effects (slight differences in geometry and/or in the damping properties among blades [10, 11]) were neglected in the performed analyses. Under these conditions, the disc assembly is a rotationally periodic structure of N identical blades and the cyclic wave theory may be applied. When dealing with bladed discs, gyroscopic effects are usually neglected. Thus, the static and dynamic deformations of the whole disc could be represented by a single blade-disc-shaft sector with complex circumferential boundary conditions.

Neglecting dissipation effects, the harmonic free vibration of the system is given by the following complex matrix equation:

$$[M(e^{jk\varphi})]\{d^2q/dt^2\} + [K(e^{jk\varphi}, \Omega)]\{q\} = \{0\}, \quad j^2 = -1, \quad (1)$$

where $\varphi = 2\pi/N$ is the circumferential periodicity angle of the blade-disc-shaft sector, and the nodal diameter number k varies according to:

$$\begin{aligned} & N/2 \quad \text{for } N \text{ even,} \\ k = 0, 1, 2, \dots, (N-1)/2 \quad & \text{for } N \text{ uneven.} \end{aligned} \quad (2)$$

In Equation (1), $[M(e^{jk\varphi})]$, $[K(e^{jk\varphi}, \Omega)]$ represent the blade mass and non-linear stiffness matrices with respect to the rotational speed Ω . Both of these complex matrices depend on the nodal diameter number k . The complex vectors $\{q\}$ and $\{d^2q/dt^2\}$ describe the nodal displacement and the acceleration of the blade-disc-shaft vibration. Between nodes located on the right and left circumferential sector sides, cyclic kinematic constraints are imposed as:

$$\{q\}_{\text{right}} = \{q\}_{\text{left}} e^{jk\varphi}, \quad \{d^2q/dt^2\}_{\text{right}} = \{d^2q/dt^2\}_{\text{left}} e^{jk\varphi}. \quad (3)$$

Rewriting the Euler function in trigonometric notation, eigenfrequencies of the cyclic finite element system can be computed in the real domain. For each mode and nodal diameter k (besides $k=0$ and $k=N/2$), two identical eigenfrequencies are computed which refer to two possible orthogonal mode shapes of the disc assembly.

By substituting k equal to 0 into Equation (1) and Equations (3), as well as omitting the inertial term of Equation (1), a static equation of the disc assembly rotating with the angular speed Ω is obtained in the following form:

$$[K(\Omega)]\{q\} = \{F(\Omega)\}, \quad (4)$$

where $[K(\Omega)]$ is the stiffness matrix, and $\{F(\Omega)\}$ is the centrifugal force. In our case, the blades can be circumferentially coupled by a shroud, blades, discs, or shaft. In this case, any contact area between the blade and shroud is obtained. Finally, for the considered rotational speed Ω , eigenfrequencies of the shrouded bladed discs can be computed.

3. Numerical model and experimental validation

The structure is composed of 144 shrouded blades, mounted rigidly (see Figure 1) on a supported disc. The main dimensions are as follows: disc-outer

diameter=0.685m, inner diameter=0.196m, height of the blade=0.159m. According to the theoretical model, only 1/144th of the bladed disc assembly is meshed, isoparametric brick elements with 20 nodes and 3 degrees of freedom per node are used (1112 elements for a bladed disc). Natural frequencies of a rotating shrouded bladed disc have been calculated.

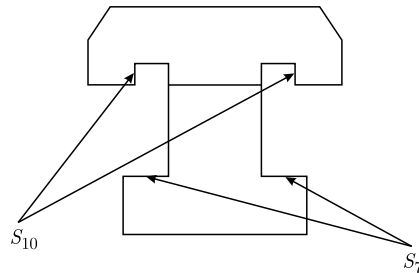


Figure 1. Cross section of a blade root (S_7 , S_{10} are the contact areas of the blade to the disc)

The non-dimensional numerical results computed for all the possible nodal diameters are reported on the Interference diagram presented in Figure 2 and in Table 1. The modes of the bladed disc are classified by analogy with axisymmetric modes, which are mainly characterized by nodal lines lying along the diameters of the structure and having constant angular spacing. There are either zero ($k=0$), one ($k=1$), two ($k=2$), or more ($k>2$) nodal diameter bending or torsion modes. Series 1 is associated with the first natural frequency of the single cantilever blade. Series 2 is associated with the second natural frequency of the single cantilever blade, and so on (k is the number of nodal diameters).

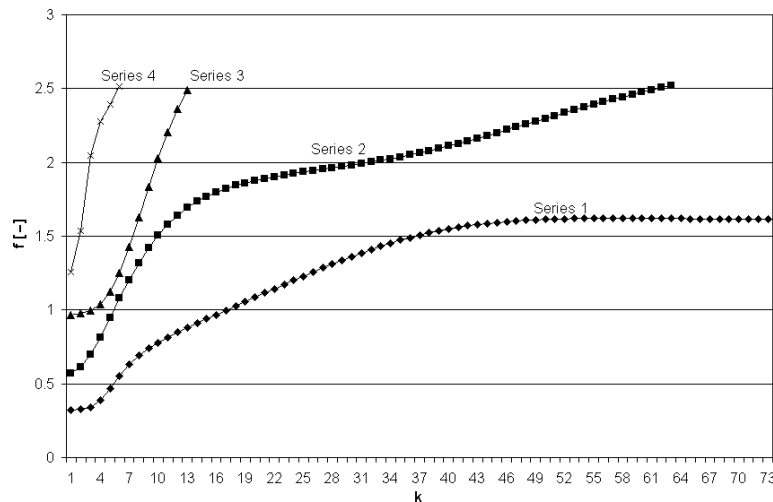


Figure 2. Interference diagram of a shrouded bladed disc

Next, the natural frequencies of a shrouded bladed disc placed on the part of a shaft (see Figure 3) were calculated.

The non-dimensional natural frequencies computed for all the possible nodal diameters are reported on the interference diagram presented in Figure 4 and in

Table 1. Non-dimensional natural frequencies of a shrouded bladed disc for temperature 150°C and speed of rotation $n = 3000$ rpm

| k | Series 1 | Series 2 | Series 3 | Series 4 |
|-----|----------|----------|----------|----------|
| 0 | 0.322855 | 0.569566 | 0.968552 | 1.259793 |
| 1 | 0.325359 | 0.610572 | 0.975931 | 1.537655 |
| 2 | 0.341503 | 0.699862 | 0.996069 | 2.046897 |
| 3 | 0.388366 | 0.816069 | 1.040138 | 2.278069 |
| 4 | 0.466917 | 0.946207 | 1.122069 | 2.393655 |
| 5 | 0.554745 | 1.078414 | 1.252897 | 2.512414 |
| 6 | 0.631083 | 1.203862 | 1.429103 | |
| 7 | 0.691241 | 1.318414 | 1.630552 | |
| 8 | 0.739103 | 1.419793 | 1.835517 | |
| 9 | 0.779241 | 1.507172 | 2.029586 | |
| 10 | 0.814759 | 1.580759 | 2.205379 | |
| 11 | 0.847517 | 1.642 | 2.359862 | |
| 12 | 0.87869 | 1.692621 | 2.492345 | |
| 13 | 0.908966 | 1.734414 | | |
| 14 | 0.93869 | 1.769103 | | |
| 15 | 0.968138 | 1.798069 | | |
| 16 | 0.997517 | 1.822483 | | |
| 17 | 1.026828 | 1.843241 | | |
| 18 | 1.056138 | 1.861172 | | |
| 19 | 1.085379 | 1.876759 | | |
| 20 | 1.114621 | 1.890552 | | |

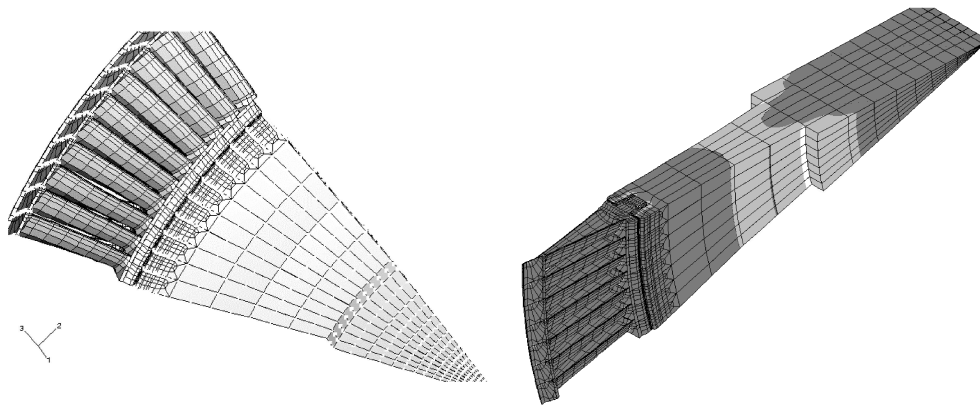
**Figure 3.** A shrouded bladed disc with the part of the shaft

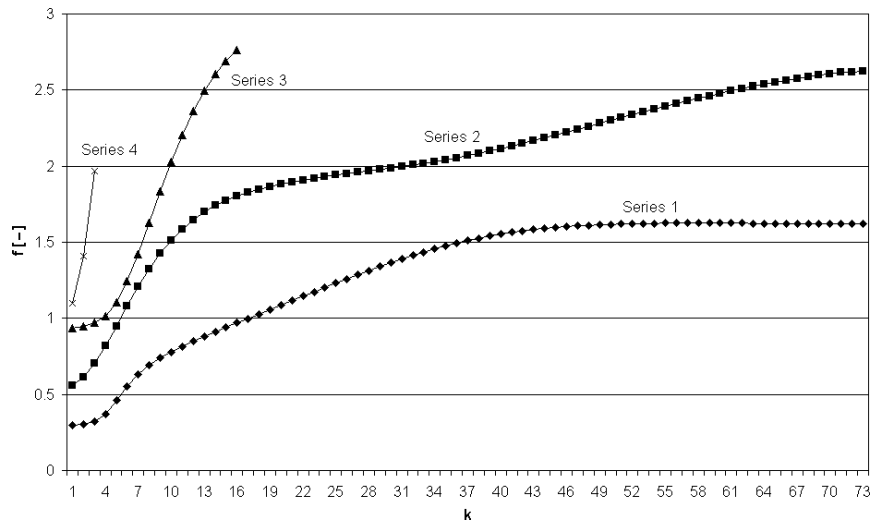
Table 2. Series 1 is associated with the first natural frequency of the single cantilever blade. Series 2 is associated with the second natural frequency of the single cantilever blade, and so on (k is the number of nodal diameters).

The non-dimensional natural frequencies of a shrouded bladed disc and of a shrouded bladed disc with the part of the shaft are presented in Table 3 and Figure 5.

In Figure 5 symbol 'se1zwal' is associated with Series 1 of a shrouded bladed disc with the part of the shaft, and the symbol 'se2zwal' is associated with Series 2

Table 2. Non-dimensional natural frequencies of a shrouded bladed disc with the part of the shaft for temperature 150°C and speed of rotation $n = 3000$ rpm

| k | Series 1 | Series 2 | Series 3 | Series 4 |
|-----|----------|----------|----------|----------|
| 0 | 0.299476 | 0.561655 | 0.934414 | 1.096276 |
| 1 | 0.301931 | 0.611676 | 0.945931 | 1.411241 |
| 2 | 0.319821 | 0.703103 | 0.968897 | 1.969448 |
| 3 | 0.372862 | 0.819172 | 1.017172 | |
| 4 | 0.459276 | 0.949379 | 1.104828 | |
| 5 | 0.55231 | 1.081862 | 1.242069 | |
| 6 | 0.630766 | 1.207655 | 1.423862 | |
| 7 | 0.691586 | 1.322483 | 1.62869 | |
| 8 | 0.739655 | 1.424207 | 1.835241 | |
| 9 | 0.779931 | 1.511862 | 2.029862 | |
| 10 | 0.815517 | 1.585724 | | |
| 11 | 0.848276 | 1.647172 | | |
| 12 | 0.879517 | 1.698 | | |
| 13 | 0.909793 | 1.739931 | | |
| 14 | 0.939517 | 1.774759 | | |
| 15 | 0.969034 | 1.803793 | | |
| 16 | 0.998414 | 1.828276 | | |
| 17 | 1.027793 | 1.849103 | | |
| 18 | 1.057103 | 1.867034 | | |
| 19 | 1.086414 | 1.882621 | | |
| 20 | 1.115724 | 1.896414 | | |

**Figure 4.** Interference diagram of a shrouded bladed disc with the part of the shaft

of a shrouded bladed disc with the part of the shaft, and the symbol 'sell144' is associated with Series 1 of a shrouded bladed disc without the part of the shaft.

The natural frequencies of a shrouded bladed disc with the part of the shaft are generally lower than the natural frequencies of a shrouded bladed disc without

Table 3. Non-dimensional natural frequencies of a shrouded bladed disc and shrouded bladed disc with the part of the shaft for temperature 150°C and speed of rotation $n = 3000$ rpm

| k | Natural frequencies | | | |
|-----|----------------------------|----------|---------------|----------|
| | With the part of the shaft | | Without shaft | |
| | Series 1 | Series 2 | Series 1 | Series 2 |
| 0 | 0.2994 | 0.5616 | 0.3228 | 0.5695 |
| 1 | 0.3019 | 0.6116 | 0.3253 | 0.6105 |
| 2 | 0.3198 | 0.7031 | 0.3415 | 0.6998 |
| 3 | 0.3728 | 0.8191 | 0.3888 | 0.8160 |
| 4 | 0.4592 | 0.9493 | 0.4669 | 0.9462 |
| 5 | 0.5523 | 1.0818 | 0.5547 | 1.0784 |
| 6 | 0.6307 | 1.2076 | 0.6310 | 1.2038 |
| 7 | 0.6915 | 1.3224 | 0.6912 | 1.3184 |
| 8 | 0.7396 | 1.4242 | 0.7391 | 1.4197 |
| 9 | 0.7799 | 1.5118 | 0.7792 | 1.5071 |
| 10 | 0.8155 | 1.5857 | 0.8147 | 1.5807 |

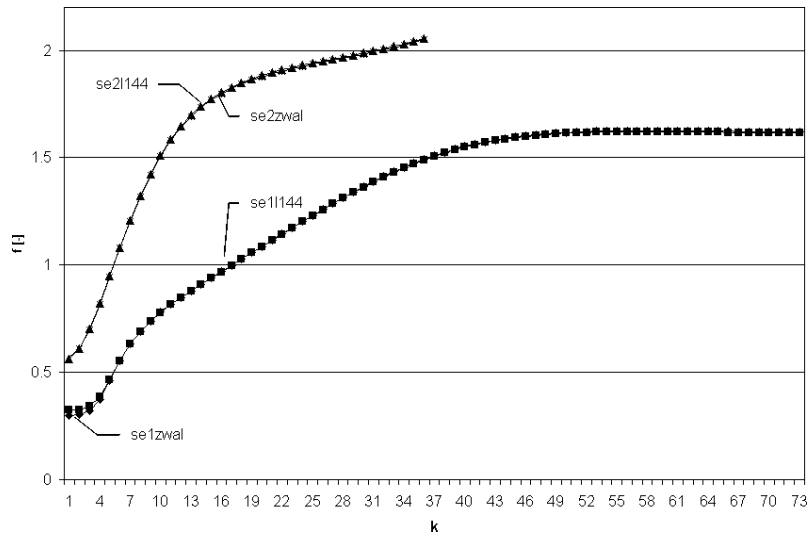


Figure 5. Interference diagram of a shrouded bladed disc with the part of the shaft and without the shaft

the part of the shaft, for nodal diameter modes of Series 1 through 6 (see Figure 5 and Table 3). However, for nodal diameter modes greater than seven the frequencies are greater (see Table 3). In Series 2 (see Table 3), only the first frequency of two shrouded bladed discs placed on the shaft is lower than the corresponding natural frequency of one shrouded bladed disc without the shaft.

In Figure 6, the symbol 'se12wal' is associated with Series 1 of a shrouded bladed disc with the part of the shaft, and the symbol 'se11144' is associated with Series 1 of a shrouded bladed disc without the part of the shaft.

During the experimental test, measurements of natural frequencies at rest were obtained for a bladed discs placed on the shaft. The measurements were made for a speed of rotation 0rpm and temperature 20°C. The measured values are shown

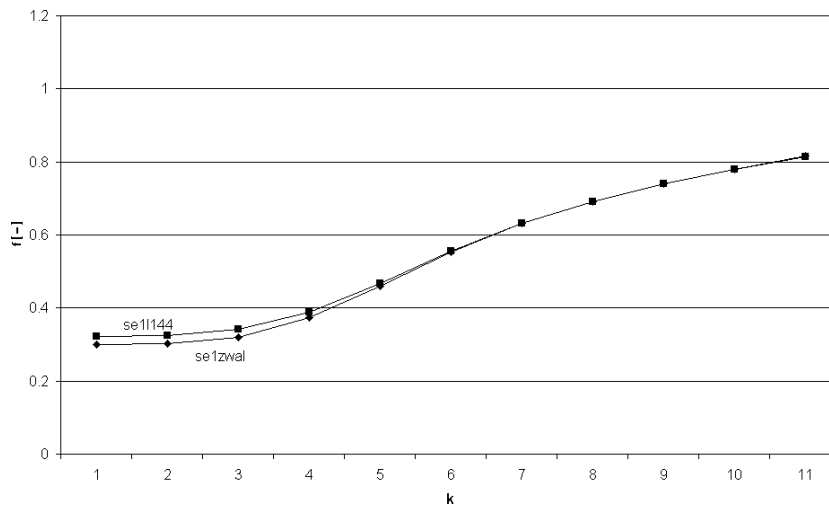


Figure 6. Interference diagram of a shrouded bladed disc with the part of the shaft and without the shaft for the first series of frequencies

in Table 4, and compared with the associated numerical values. The comparison illustrates the quality of the model when the part of the shaft is taken into account. The numerical and experimental frequencies at rest are in good agreement. Due to gyroscopic effects, the frequencies are capable of splitting into backward and forward branches. In our case, gyroscopic effects are neglected, so the natural frequencies are doubled for $k > 0$ and $k < N/2$.

Subsequently, the natural frequencies of the two shrouded bladed discs placed on the shaft (see Figure 7) were calculated. The natural frequencies of the two shrouded bladed discs with the part of the shaft are presented in Table 5 and Figure 7. Series 1 Disc 1 (see Table 5) is associated with the first natural frequency of a single cantilever blade and corresponds to the first bladed disc. Series 1 Disc 2 is associated with the first natural frequency of a single cantilever blade and corresponds to the second bladed disc. Series 2 Disc 1 is associated with the second natural frequency of a single cantilever blade and corresponds to the first bladed disc, and so on (k is the number of nodal diameters).

Series 1 (see Figure 7) is associated with the first natural frequency of a single cantilever blade and corresponds to the first bladed disc. Series 2 is associated with the first natural frequency of a single cantilever blade and corresponds to the second bladed disc. Series 3 is associated with the second natural frequency of a single cantilever blade and corresponds to the first bladed disc, and so on (k is the number of nodal diameters).

The spectrum of the non-dimensional natural frequencies of two bladed discs placed on the shaft is divided into the natural frequencies corresponding to the vibration of the first bladed disc and the natural frequencies corresponding to the vibration of the second bladed disc. The differences between the natural frequencies of the first bladed disc and the second bladed disc for the Series 1, corresponding to the first natural frequencies of the single blade, are small, but the mode shapes are different. At frequency 0.292 (see Table 5, Series 1 Disc 2 $k = 0$ and Figure 8a),

Table 4. Measured and calculated non-dimensional natural frequencies of a shrouded bladed disc and a shrouded bladed disc with the part of the shaft for temperature 20°C and speed of rotation $n = 0$ rpm

| k | CALCULATION | | EXPERIMENT |
|-----|-------------|---------------|-------------|
| | With shaft | Without shaft | |
| 0 | 0.304 | 0.324 | 0.258–0.268 |
| 1 | 0.307 | 0.327 | 0.279–0.281 |
| 2 | 0.326 | 0.343 | — |
| 3 | 0.381 | 0.390 | 0.319–0.326 |
| 4 | 0.472 | 0.470 | 0.386–0.392 |
| 5 | 0.573 | 0.559 | 0.455–0.458 |
| 6 | 0.660 | 0.636 | 0.524–0.527 |
| 7 | 0.748 | 0.696 | 0.574–0.588 |
| 8 | 0.825 | 0.744 | 0.643–0.651 |
| 9 | 0.903 | 0.785 | 0.706–0.720 |
| 10 | 0.986 | 0.820 | 0.794–0.797 |
| 11 | 1.075 | 0.853 | 0.861–0.886 |
| 12 | 1.170 | 0.885 | 0.908–0.941 |
| 13 | 1.270 | 0.915 | 0.971–0.982 |
| 14 | 1.374 | 0.945 | 1.059–1.070 |
| 15 | 1.481 | 0.975 | 1.103–1.106 |
| 16 | 1.586 | 1.004 | 1.150–1.170 |
| 17 | 1.687 | 1.034 | 1.263–1.283 |

the second bladed disc vibrates with the relative amplitude 1.0 and the first bladed disc vibrates with the amplitude 0.834. At frequency 0.297 (see Table 5, Series 1 Disc 1 $k = 0$), the first bladed disc vibrates with the relative amplitude 1.0 and the second bladed disc vibrates with the amplitude 0.95. At frequency 0.2935, $k = 1$ (see Figure 8a), the second bladed disc vibrates with the amplitude 1.108 and the first bladed disc vibrates with the amplitude 0.923.

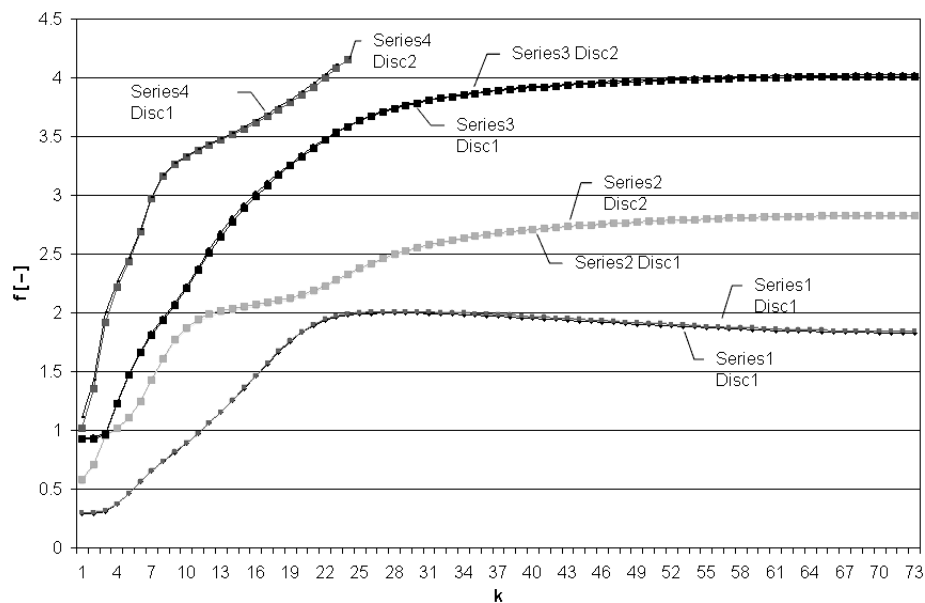
At a non-dimensional frequency 0.3117 (see Table 5, Series 1 Disc 2 $k = 2$ and Figure 8b), the second bladed disc vibrates with the relative amplitude 1.055 and the first bladed disc vibrates with the relative amplitude 0.791. At frequency 0.464 (see Table 5, Series 1 Disc 1 $k = 4$ and Figure 8b), the first bladed disc vibrates with the relative amplitude 1.0, and the second bladed disc vibrates with the relative amplitude 0.0912. In the case of mode shapes corresponding to nodal diameters greater than four, only one bladed disc is vibrating (see Figure 8c) and differences between natural frequencies are very small (see Table 5).

For Series 2 (Table 5, Series 2 Disc 2 and Series 2 Disc 1), the differences between frequencies in the considered group are greater, and the influence of one bladed disc on the other is similar to that of the first group (see Figure 9). For the higher series of bladed disc frequencies, the influence of bladed discs on each other are different. Generally, natural frequencies of two shrouded bladed discs are greater than those of one shrouded bladed disc, except for a few first modes (see Table 5 and Table 3).

Thus, the natural frequencies of three shrouded bladed discs placed on the shaft (see Figure 11a) were calculated. The natural frequencies of two and three

Table 5. Non-dimensional natural frequencies of two shrouded bladed discs with the part of the shaft for temperature 150°C and speed of rotation $n = 3000\text{rpm}$

| k | Series 1 | | Series 2 | | Series 3 | | Series 4 | |
|-----|----------|--------|----------|--------|----------|--------|----------|--------|
| | Disc 2 | Disc 1 | Disc 2 | Disc 1 | Disc 2 | Disc 1 | Disc 2 | Disc 1 |
| 0 | 0.292 | 0.297 | 0.564 | 0.5775 | 0.923 | 0.929 | 1.0217 | 1.105 |
| 1 | 0.2935 | 0.300 | 0.699 | 0.7072 | 0.9317 | 0.942 | 1.3536 | 1.4266 |
| 2 | 0.3117 | 0.318 | 0.950 | 0.9573 | 0.9606 | 0.970 | 1.9194 | 2.0042 |
| 3 | 0.3686 | 0.373 | 1.009 | 1.0173 | 1.227 | 1.236 | 2.2163 | 2.2681 |
| 4 | 0.461 | 0.464 | 1.102 | 1.1088 | 1.47 | 1.480 | 2.4325 | 2.463 |
| 5 | 0.5623 | 0.565 | 1.242 | 1.2477 | 1.6641 | 1.676 | 2.6901 | 2.7075 |
| 6 | 0.6541 | 0.657 | 1.415 | 1.4239 | 1.8133 | 1.826 | 2.9689 | 2.9774 |
| 7 | 0.7352 | 0.738 | 1.596 | 1.6093 | 1.937 | 1.951 | 3.1665 | 3.1712 |
| 8 | 0.8119 | 0.815 | 1.751 | 1.7682 | 2.0616 | 2.077 | 3.267 | 3.2718 |
| 9 | 0.8894 | 0.893 | 1.858 | 1.8768 | 2.2054 | 2.225 | 3.3317 | 3.3373 |
| 10 | 0.9714 | 0.975 | 1.924 | 1.9434 | 2.3603 | 2.385 | 3.382 | 3.3889 |
| 11 | 1.0592 | 1.063 | 1.968 | 1.9867 | 2.5108 | 2.540 | 3.4271 | 3.4359 |
| 12 | 1.153 | 1.157 | 1.998 | 2.0171 | 2.6497 | 2.681 | 3.4714 | 3.4824 |
| 13 | 1.2523 | 1.256 | 2.021 | 2.0402 | 2.775 | 2.806 | 3.5169 | 3.5308 |
| 14 | 1.3555 | 1.36 | 2.040 | 2.0588 | 2.8874 | 2.917 | 3.5648 | 3.5817 |
| 15 | 1.4605 | 1.465 | 2.056 | 2.075 | 2.9889 | 3.016 | 3.6154 | 3.6353 |
| 16 | 1.5646 | 1.569 | 2.072 | 2.0903 | 3.0819 | 3.106 | 3.669 | 3.6917 |
| 17 | 1.6645 | 1.669 | 2.088 | 2.1068 | 3.1686 | 3.189 | 3.7258 | 3.751 |
| 18 | 1.7559 | 1.761 | 2.108 | 2.1264 | 3.2506 | 3.267 | 3.7864 | 3.8136 |
| 19 | 1.8341 | 1.840 | 2.134 | 2.1523 | 3.3286 | 3.342 | 3.8518 | 3.8803 |
| 20 | 1.894 | 1.901 | 2.17 | 2.187 | 3.402 | 3.413 | 3.922 | 3.9521 |

**Figure 7.** Interference diagram of two shrouded bladed discs with the part of the shaft

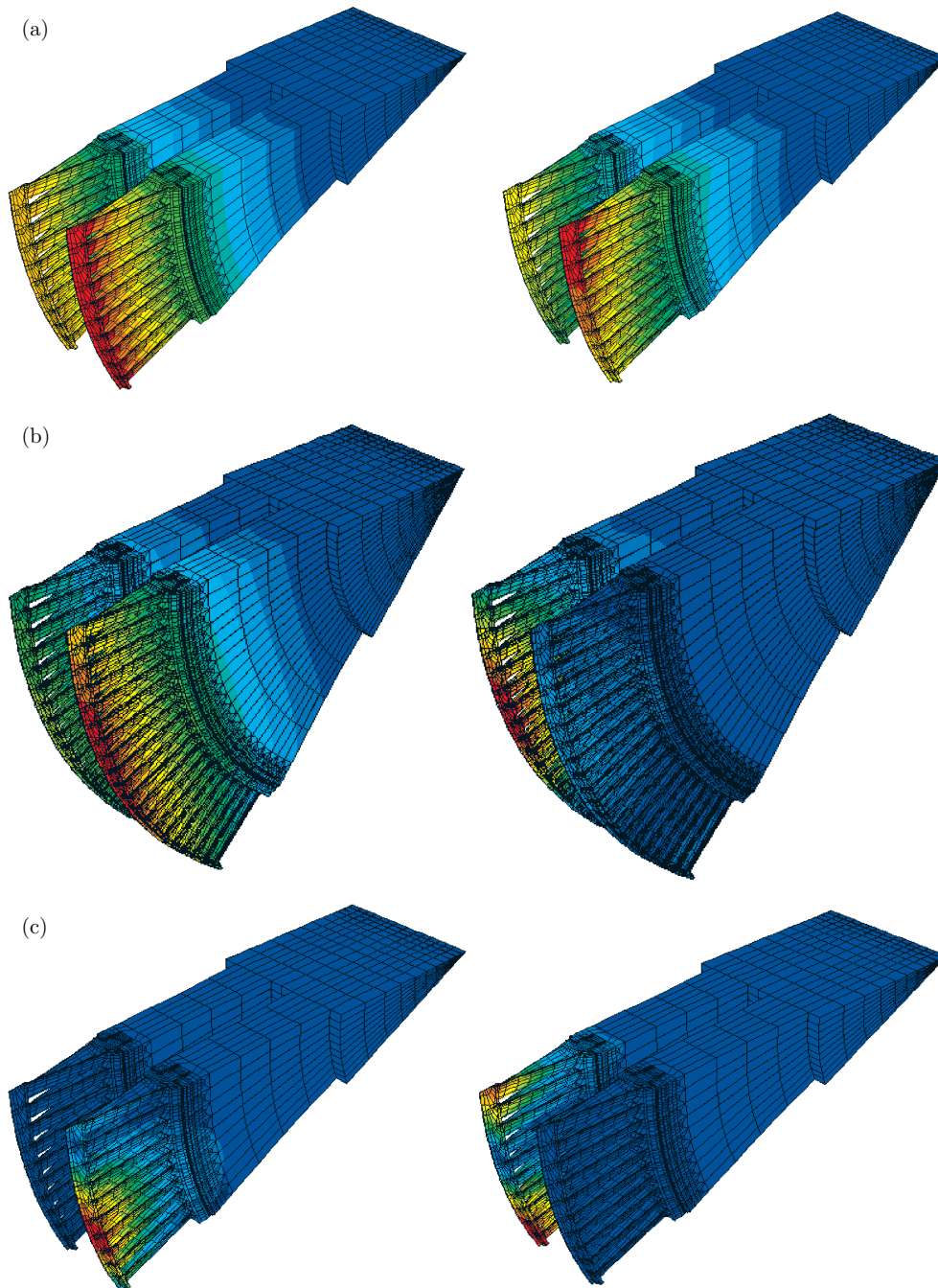


Figure 8. (a) Mode shapes of two shrouded bladed discs placed on the shaft for the first group: on the left – Disc 2, $f = 0.292$, $k = 0$; on the right – Disc 1, $f = 0.2935$, $k = 1$. (b) Mode shapes of two shrouded bladed discs placed on the shaft for the first group: on the left – Disc 2, $f = 0.3117$, $k = 2$; on the right – Disc 1, $f = 0.464$, $k = 4$. (c) Mode shapes of two shrouded bladed discs placed on the shaft for the first group: on the left – Disc 2, $f = 0.7352$, $k = 7$; on the right – Disc 1, $f = 0.738$, $k = 7$

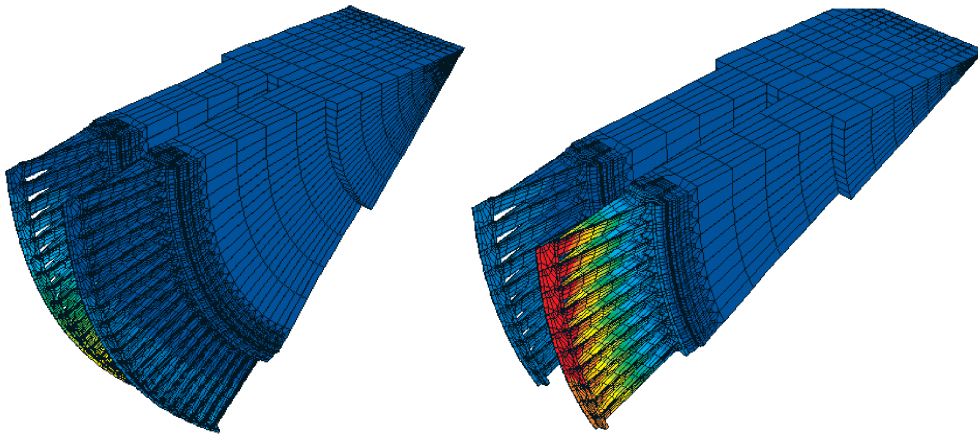


Figure 9. Mode shapes of two shrouded bladed discs placed on the shaft for the second group: on the left – Disc 2, $f = 0.699$, $k = 1$; on the right – Disc 1, $f = 0.7072$, $k = 1$

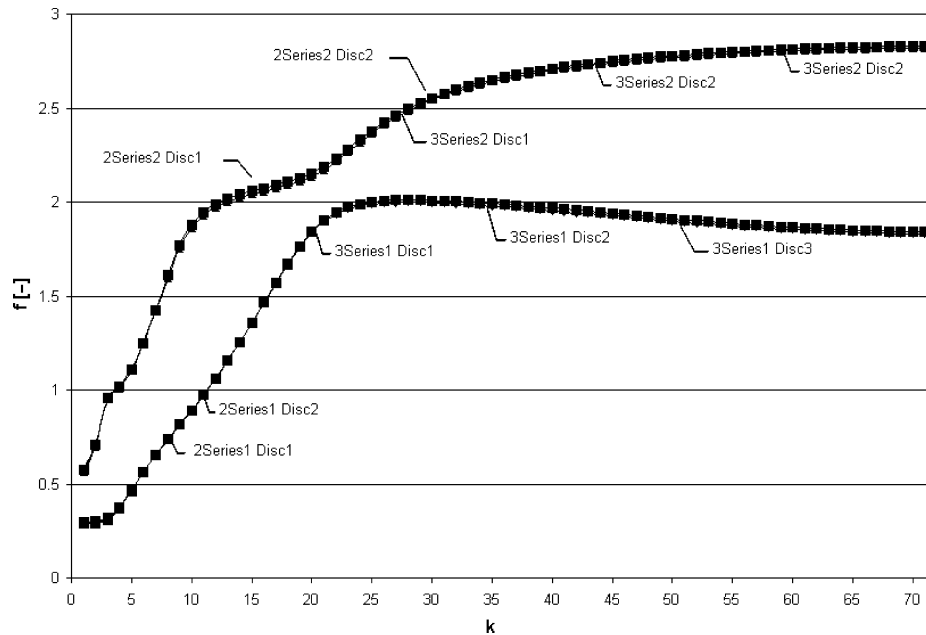


Figure 10. Interference diagram of two shrouded bladed discs with the part of the shaft and three shrouded bladed discs with the part of the shaft

shrouded bladed discs with the part of the shaft are presented in Table 6 and Figures 11a–11d, 12a and 12b. Series 1 Disc 1 is associated with the first natural frequency of a single cantilever blade and corresponds to the first bladed disc. Series 1 Disc 2 is associated with the first natural frequency of a single cantilever blade and corresponds to the second bladed disc. Series 1 Disc 3 is associated with the first natural frequency of a single cantilever blade and corresponds to the third bladed disc. Series 2 Disc 1 is associated with the second natural frequency of a single cantilever blade and corresponds to the first bladed disc, and so on (k is the number of nodal diameters). The symbol ‘2Series1 Disc1’ (see Figure 10) is associated with the first

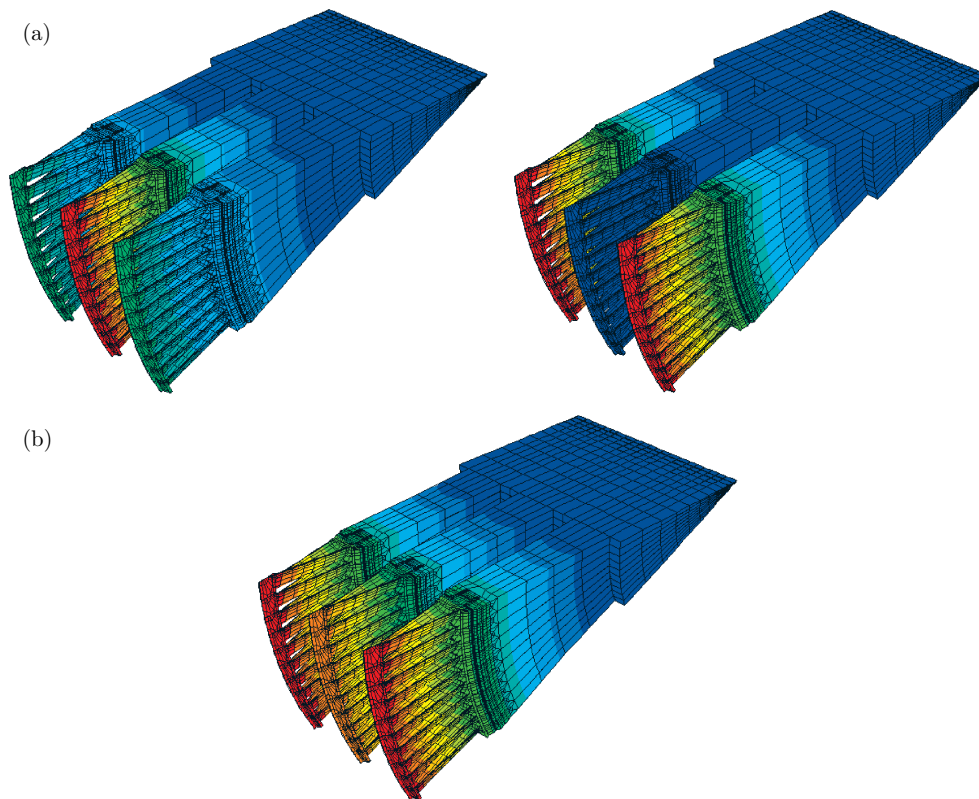


Figure 11. (a) Mode shapes of three shrouded bladed discs placed on the shaft for the first group: on the left – Disc 1, $f=0.2901$, $k=0$; on the right – Disc 3, $f=0.2956$, $k=0$.
 (b) Mode shape of three shrouded bladed discs placed on the shaft for the first group: Disc 2, $f=0.2984$, $k=0$ (continued on the next page)

natural frequency of a single cantilever blade and corresponds to the first of the two bladed discs. In the interference diagram (see Figure 10), ‘2Series1 Disc2’ is associated with the first natural frequency of a single cantilever blade and corresponds to the second of the two bladed discs. ‘2Series2 Disc1’ is associated with the second natural frequency of a single cantilever blade and corresponds to the first of the two bladed discs, and so on (k is the number of nodal diameters). ‘3Series1 Disc1’ is associated with the first natural frequency of a single cantilever blade and corresponds to the first of the three bladed discs. ‘3Series1 Disc2’ is associated with the first natural frequency of a single cantilever blade and corresponds to the second of the three bladed discs. ‘3Series1 Disc3’ is associated with the first natural frequency of a single cantilever blade and corresponds to the third of the three bladed discs. ‘3Series2 Disc1’ is associated with the second natural frequency of a single cantilever blade and corresponds to the first of the three bladed discs, and so on (k is the number of nodal diameters).

At a non-dimensional frequency 0.2901 (see Table 6, Series 1 Disc 1 $k=0$ and Figure 11a), the second bladed disc is vibrating with the relative amplitude 1.0 and the first and the third bladed discs are vibrating with the relative amplitude 0.670. At frequency 0.2956 (see Table 6, Series 1 Disc 3 $k=0$ and Figure 11a), the first and

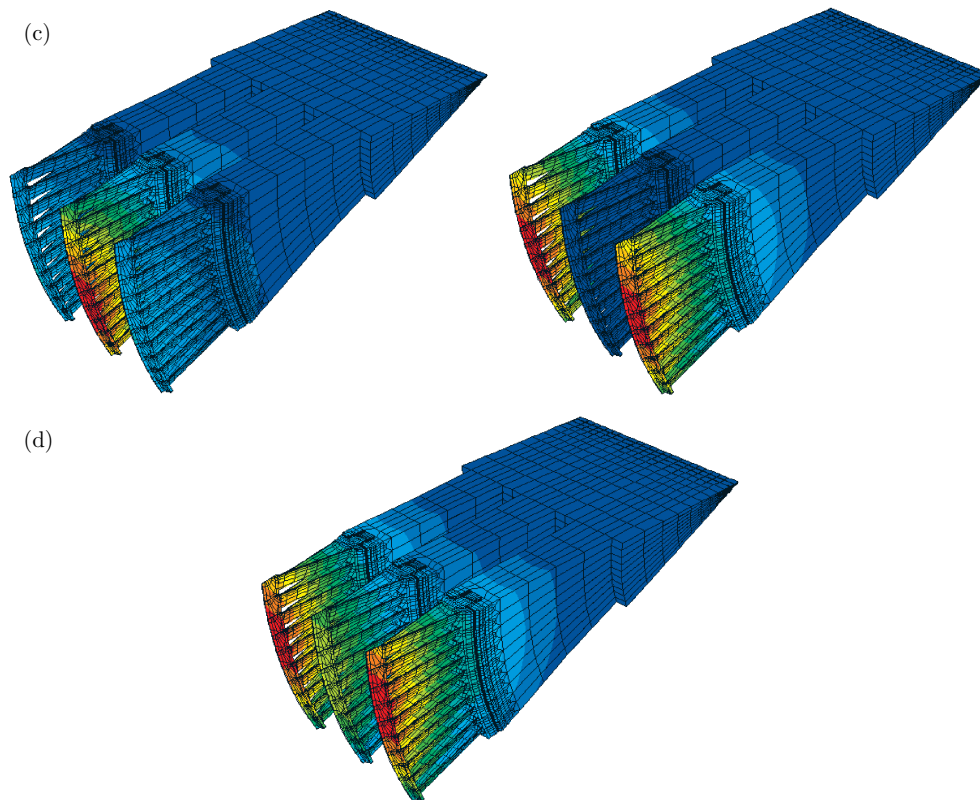


Figure 11 – continued. (c) Mode shapes of three shrouded bladed discs placed on the shaft for the first group: on the left – Disc 1, $f = 0.4622$, $k = 0$; on the right – Disc 3, $f = 0.4637$, $k = 0$.
 (d) Mode shape of three shrouded bladed discs placed on the shaft for the first group:
 Disc 2, $f = 0.4643$, $k = 4$

the third bladed discs are vibrating. At frequency 0.2984, $k = 0$ (see Figure 11b), all three bladed discs are vibrating: the first and the third – with a relative amplitude of 1.0 and the second – with an amplitude of 0.918.

At a non-dimensional frequency 0.4622 (see Table 6, Series 1 Disc 1 $k = 4$ and Figure 11c), the third bladed disc is vibrating with the relative amplitude 1.0 and the first and the second bladed discs are vibrating with the amplitude 0.352. At frequency 0.4637 (see Table 6, Series 1 Disc 3 $k = 4$ and Figure 11c), the first and the third bladed discs are vibrating. At frequency 0.4643, $k = 4$ (see Figure 11d), three bladed discs are vibrating: the first and the third bladed discs – with an amplitude of 1.0 and the second – with an amplitude of 0.584.

In the case of mode shapes corresponding to nodal diameters greater than four, only one bladed disc is vibrating (see Figures 12a and 12b), and differences between natural frequencies are very small (see Table 6).

For Series 2, the differences among frequencies in the considered series are greater and the influence of the one bladed disc on the second and the third is similar to that in Series 1. For the higher series of bladed disc frequencies, the influence of bladed discs on each other is different. Generally, natural frequencies of three shrouded

Table 6. Non-dimensional natural frequencies of two and three shrouded bladed discs with the part of the shaft for temperature 150°C and speed of rotation $n = 3000$ rpm

| k | Two bladed discs | | | | Three bladed discs | | | | | |
|----|------------------|--------|----------|--------|--------------------|--------|--------|----------|--------|--------|
| | Series 1 | | Series 2 | | Series 1 | | | Series 2 | | |
| | Disc 2 | Disc 1 | Disc 2 | Disc 1 | Disc 1 | Disc 3 | Disc 2 | Disc 1 | Disc 3 | Disc 2 |
| 0 | 0.292 | 0.2979 | 0.5647 | 0.5775 | 0.2901 | 0.2956 | 0.2984 | 0.5446 | 0.5760 | 0.5799 |
| 1 | 0.2935 | 0.3003 | 0.6999 | 0.7072 | 0.2923 | 0.2962 | 0.3008 | 0.7022 | 0.7074 | 0.7083 |
| 2 | 0.3117 | 0.3184 | 0.9503 | 0.9573 | 0.3111 | 0.3153 | 0.3190 | 0.9532 | 0.9568 | 0.9588 |
| 3 | 0.3686 | 0.3732 | 1.009 | 1.0173 | 0.3686 | 0.3720 | 0.3737 | 1.0103 | 1.0159 | 1.0180 |
| 4 | 0.461 | 0.464 | 1.1028 | 1.1088 | 0.4622 | 0.4637 | 0.4643 | 1.1043 | 1.1083 | 1.1092 |
| 5 | 0.5623 | 0.5651 | 1.2421 | 1.2477 | 0.5647 | 0.5651 | 0.5652 | 1.2455 | 1.2475 | 1.2479 |
| 6 | 0.6541 | 0.6572 | 1.4159 | 1.4239 | 0.6571 | 0.6572 | 0.6572 | 1.4231 | 1.4238 | 1.4240 |
| 7 | 0.7352 | 0.7386 | 1.5969 | 1.6093 | 0.7386 | 0.7386 | 0.7386 | 1.6092 | 1.6093 | 1.6094 |
| 8 | 0.8119 | 0.8154 | 1.7516 | 1.7682 | 0.8153 | 0.8153 | 0.8154 | 1.7682 | 1.7682 | 1.7683 |
| 9 | 0.8894 | 0.8931 | 1.8582 | 1.8768 | 0.8930 | 0.8930 | 0.8932 | 1.8767 | 1.8767 | 1.8768 |
| 10 | 0.9714 | 0.9751 | 1.9248 | 1.9434 | 0.9751 | 0.9751 | 0.9752 | 1.9434 | 1.9434 | 1.9434 |
| 11 | 1.0592 | 1.0631 | 1.9681 | 1.9867 | 1.0630 | 1.0630 | 1.0632 | 1.9866 | 1.9866 | 1.9867 |
| 12 | 1.153 | 1.1571 | 1.9987 | 2.0171 | 1.1571 | 1.1571 | 1.1572 | 2.0171 | 2.0171 | 2.0172 |
| 13 | 1.2523 | 1.2566 | 2.0219 | 2.0402 | 1.2566 | 1.2566 | 1.2567 | 2.0402 | 2.0402 | 2.0402 |
| 14 | 1.3555 | 1.36 | 2.0406 | 2.0588 | 1.3599 | 1.3599 | 1.3601 | 2.0588 | 2.0588 | 2.0588 |
| 15 | 1.4605 | 1.4652 | 2.0568 | 2.075 | 1.4652 | 1.4652 | 1.4653 | 2.0750 | 2.0750 | 2.0750 |
| 16 | 1.5646 | 1.5695 | 2.0721 | 2.0903 | 1.5694 | 1.5695 | 1.5696 | 2.0903 | 2.0903 | 2.0903 |

bladed discs are greater than those of one shrouded bladed disc, except for a few first modes (see Table 6 and Table 3).

It follows from presented results that the spectrum of natural frequencies of three bladed discs placed on the shaft is divided into the natural frequencies corresponding to the vibration of the first bladed disc (see '3Series1 Disc1', '3Series2 Disc1', Figures 10, 11a–11d, 12a and 12b), the natural frequencies corresponding to the vibration of the second bladed disc (see '3Series1 Disc2', '3Series2 Disc2', Figures 10, 11a–11d, 12a and 12b), and the natural frequencies corresponding to the vibration of the third bladed disc (see '3Series1 Disc3', '3Series2 Disc3', Figures 10, 11a–11d, 12a and 12b). The differences between the natural frequencies of the first, the second and the third bladed disc for the Series 1 corresponding to the first natural frequencies of a single blade are very small. In modes Series 1 Disc 1 ($f = 0.5647$ – 1.5694), Series 1 Disc 3 ($f = 0.5651$ – 1.5695), Series 1 Disc 2 ($f = 0.5652$ – 1.5696) and Series 2 Disc 1 ($f = 1.2455$ – 2.0903), Series 2 Disc 3 ($f = 1.2475$ – 2.0903), Series 2 Disc 2 ($f = 1.2479$ – 2.0903) only one bladed disc is vibrating (see Figures 12a and 12b) when the number of nodal diameters is greater than four. In the case of modes with diameter modes of less than five, the influence of the shaft is considerable and bladed discs influence each other. For higher series, the differences between natural frequencies are greater and the influence of the first bladed disc on the second and the third is visible in mode shape. Generally, the natural frequencies are greater in the case of three bladed discs in comparison to two bladed discs, except for a few first modes (see Table 6).

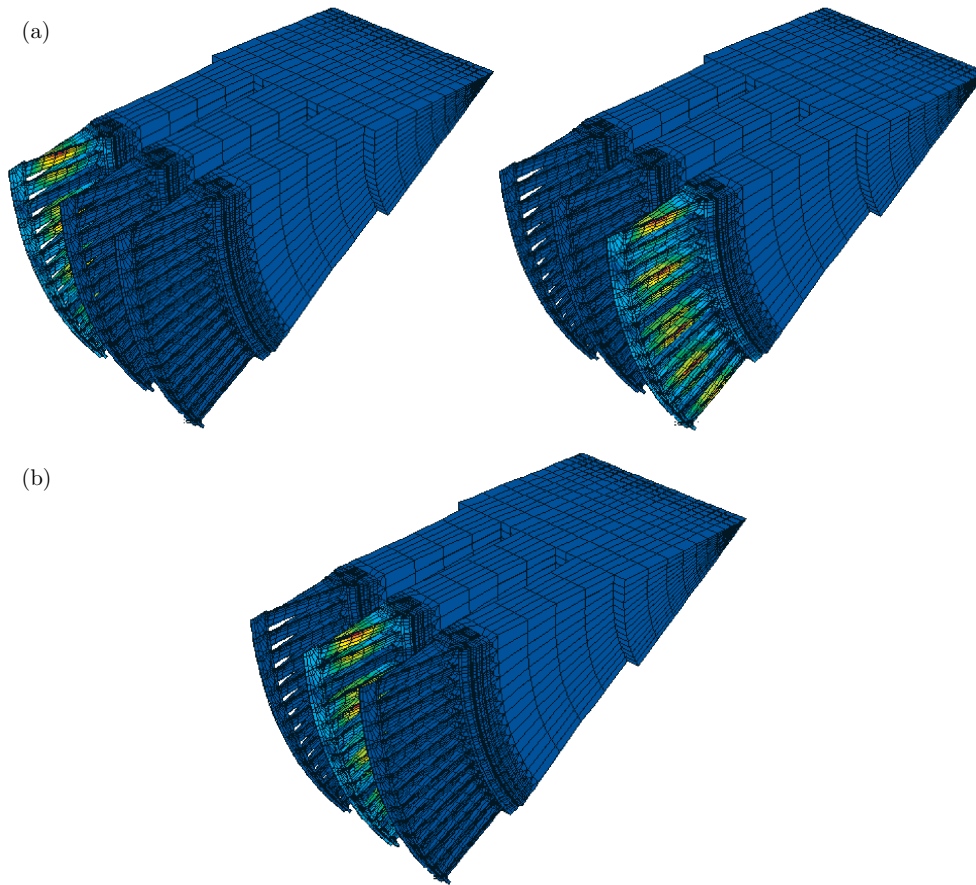


Figure 12. (a) Mode shapes of three shrouded bladed discs placed on the shaft for the first group: on the left – Disc 1, $f = 0.5694$, $k = 16$; on the right – Disc 3, $f = 0.5695$, $k = 16$. (b) Mode shape of three shrouded bladed discs placed on the shaft for the first group: Disc 2, $f = 1.5696$, $k = 16$

4. Conclusions

In this paper the natural frequencies of a rotating single shrouded bladed disc, a shrouded bladed disc placed on the part of the shaft, two and three shrouded bladed discs placed on the part of the shaft have been presented. The calculations show the influence of the shaft on the natural frequencies of the shrouded bladed discs. The inclusion of the shaft in the model modifies the interference diagram and mode shapes, which is important from the designer's point of view. The influence of shaft flexibility on mode shapes up to four nodal diameters is visible. For these modes the natural frequencies of the bladed discs with the part of the shaft are smaller than corresponding modes of the bladed disc without the shaft.

Acknowledgements

The authors wish to acknowledge KBN for the financial support for this work (project 4 T10B 033 23).

All numerical calculations have been made at the Academic Computer Centre TASK (Gdansk, Poland).

References

- [1] Berger H and Kulig T S 1981 *Simulation Models for Calculating the Torsional Vibrations of Large Turbine-generator Units after Electrical System Faults*, Simens Forsch.-u.Entwickl.-Ber., Springer-Verlag **10** (4) 237
- [2] Bogacz R, Irretier H and Szolc T 1992 *Trans. ASME, J. Vibration and Acoustics* **114** 149
- [3] Chivens D R and Nelson H D 1975 *J. Engng. for Industry* **97** 881
- [4] Rao J S 1991 *Rotor Dynamics*, 2nd Edition, John Wiley & Sons
- [5] Dopkin J A and Shoup T E 1974 *Trans. ASME* **96** 1328
- [6] Dubigeon S and Michon J C 1986 *J. Sound and Vibration* **106** (1) 53
- [7] Huang S C and Ho K B 1996 *Trans. ASME* **118** 100
- [8] Shahab A A S and Thomas J 1987 *J. Sound and Vibration* **114** (3) 435
- [9] Filippov A P and Kosinow J P 1973 *Maszinowedenije* **3** 23 (in Russian)
- [10] Rao J S 1991 *Turbomachine Blade Vibration*, Wiley Eastern Limited, New Delhi
- [11] Rządkowski R 1998 *Fluid Flow Machinery* **22**, Part Two, Wrocław, Ossolineum
- [12] Loewy R G and Khader N 1984 *Am. Inst. of Aeronautic and Astronautics J.* **22** 1319
- [13] Khader N and Loewy R G 1990 *J. Sound and Vibration* **139** (3) 469
- [14] Khader N and Masoud S 1991 *J. Sound and Vibration* **149** (3) 471
- [15] Jacquet-Richardet G, Ferraris G and Rieutord P 1996 *J. Sound and Vibration* **191** (5) 901

